

## Evidence of strong antiferromagnetic coupling between localized and itinerant electrons in ferromagnetic $\text{Sr}_2\text{FeMoO}_6$

M. Tovar, M. T. Causa, and A. Butera

*Centro Atómico Bariloche and Instituto Balseiro, Comisión Nacional de Energía Atómica and Universidad Nacional de Cuyo, 8400 San Carlos de Bariloche, Río Negro, Argentina*

J. Navarro, B. Martínez, and J. Fontcuberta

*Institut de Ciència de Materials de Barcelona, Consejo Superior de Investigación Científica, E-08193 Bellaterra, Catalunya, Spain*

M. C. G. Passeggi

*Instituto de Desarrollo Tecnológico, Consejo Nacional de Investigaciones Científicas y Técnicas and Facultad de Bioquímica y Ciencias Biológicas, Universidad Nacional del Litoral, 3000 Santa Fe, Santa Fe, Argentina*

(Received 2 January 2002; published 28 June 2002)

Magnetic dc susceptibility ( $\chi$ ) and electron-spin resonance (ESR) measurements in the paramagnetic regime, are presented. We found a Curie-Weiss behavior for  $\chi(T)$  with a ferromagnetic  $\Theta = 446(5)$  K and  $\mu_{eff} = 4.72(9)\mu_B/\text{f.u.}$ , this being lower than that expected for either  $\text{Fe}^{3+}(5.9\mu_B)$  or  $\text{Fe}^{2+}(4.9\mu_B)$  ions. The ESR  $g$  factor  $g = 2.01(2)$ , is associated with  $\text{Fe}^{3+}$ . We obtained an excellent description of the experiments in terms of two interacting sublattices: the localized  $\text{Fe}^{3+}(3d^5)$  cores and the delocalized electrons. The coupled equations were solved in a mean-field approximation, assuming for the itinerant electrons a bare susceptibility independent on  $T$ . We obtained  $\chi_e^0 = 3.7 \cdot 10^{-4}$  emu/mol. We show that the reduction of  $\mu_{eff}$  for  $\text{Fe}^{3+}$  arises from the strong antiferromagnetic interaction between the two sublattices. At variance with classical ferrimagnets, we found that  $\Theta$  is ferromagnetic. Within the same model, we show that the ESR spectrum can be described by Bloch-Hasegawa-type equations. Bottleneck is evidenced by the absence of a  $g$  shift. Surprisingly, as observed in colossal magnetoresistant manganites, no narrowing effects of the ESR linewidth is detected in spite of the presence of the strong magnetic coupling. These results provide evidence that the magnetic order in  $\text{Sr}_2\text{FeMoO}_6$  does not originate in superexchange interactions, but from a different mechanism recently proposed for double perovskites.

DOI: 10.1103/PhysRevB.66.024409

PACS number(s): 75.10.-b, 76.60.Es, 75.30.Vn

The double perovskite  $\text{Sr}_2\text{FeMoO}_6$  is known as a conducting ferromagnet (or ferrimagnet) with a relatively high transition temperature,  $T_c > 400$  K, being magnetoresistant at room temperature.<sup>1</sup> The structure of  $\text{Sr}_2\text{FeMoO}_6$  is built of perovskite blocks where the transition-metal sites are alternatively occupied by Fe and Mo ions. In the simplest ionic picture, the  $\text{Fe}^{3+}(3d^5, S=5/2)$  ion was assumed to be antiferromagnetically (AFM) coupled to their six  $\text{Mo}^{5+}(4d^1, S=1/2)$  nearest neighbors, leading to a total saturation magnetization,  $M_S = 4\mu_B/\text{f.u.}$  An alternative ionic description, giving the same  $M_S$  value, assigned  $\text{Fe}^{2+}(3d^6, S=2)$  and  $\text{Mo}^{6+}(4d^0)$ , and assumed a ferromagnetic superexchange coupling between the  $\text{Fe}^{2+}$  ions. This picture was only fairly consistent with neutron-diffraction results,<sup>2</sup> which indicated  $\mu_{Fe} = 4.1(1)\mu_B$  and  $\mu_{Mo}$  between  $0.0(1)\mu_B$  and  $0.42(6)\mu_B$ . These values were intermediate between the predictions of both ionic descriptions. Mössbauer experiments<sup>3</sup> have been interpreted in terms of an intermediate valence of  $m \cong 2.6$  for the  $\text{Fe}^{m+}$  ions. Recent X-ray absorption spectroscopy (XAS) experiments<sup>4</sup> have provided site-specific direct information on this problem: Fe is in the formal trivalent state and the magnetic moment at the Mo sites is negligible. These results are in agreement with band-structure calculations<sup>1,4</sup> that predict that well-localized spin up  $t_{2g}$  and  $e_g$  Fe subbands are fully occupied. The remaining electron goes into a spin-down  $t_{2g}$  delocalized subband

formed by hybridized Mo ( $4d$ ) and Fe ( $3d$ ) orbitals, responsible for the metallicity of the material. A well-defined AFM interaction results between the itinerant electrons and the Fe localized cores, driven by the hopping of the electrons between Fe and Mo sites.<sup>4</sup>

Magnetic measurements in the paramagnetic (PM) phase should be able to provide useful evidence in order to establish the Fe and Mo valence in this compound and the possible interaction mechanisms. Niebieskikwiat *et al.*<sup>5</sup> found that the high-temperature magnetization,  $M$ , displays a non-conventional behavior, interpreted in terms of two contributions arising from localized ( $\mu_{eff} = 6.7\mu_B/\text{f.u.}$ ) and itinerant electrons, respectively. Preliminary measurements<sup>6</sup> in samples obtained under different thermal treatments have shown, for different applied fields, apparent values for  $\mu_{eff}$  varying from  $5.9\mu_B/\text{f.u.}$  to  $4.5\mu_B/\text{f.u.}$  and suggested that this behavior was nonintrinsic and due to the existence of antisite (AS) defects and to the presence of a ferromagnetic (FM) impurity.

Electron-spin resonance (ESR) experiments also help to understand the magnetic properties of these perovskites. The  $g$  value gives information on the electronic structure of the ground state of the resonant ions and the linewidth is an experimental probe of the spin dynamics. Niebieskikwiat *et al.*<sup>5</sup> observed a single ESR line whose intensity seemed to depart from a Curie-Weiss (CW) behavior and this result was interpreted in terms of a progressive delocalization of the  $\text{Fe}^{3+}$  electrons.

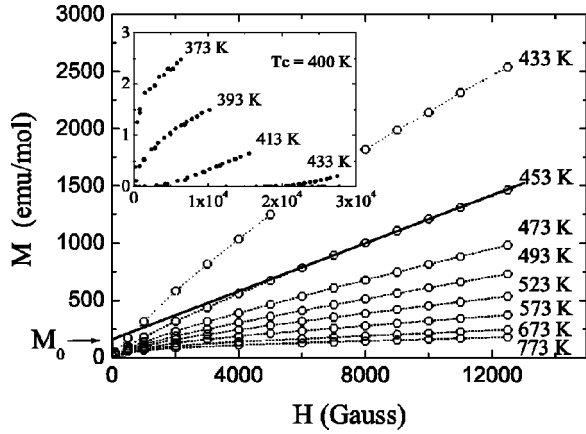


FIG. 1.  $M$  vs  $H$  at different temperatures. Inset: Arrott's plots ( $M^2$  vs  $H/M$ ) around  $T_c$ .

In this paper we present detailed dc magnetization and ESR measurements in the PM regime performed on a sample that presents an extremely low antisite defect concentration ( $A^{\text{site}} \cong 0.03$  and  $M_S = 3.7 \mu_B/\text{f.u.}$ ) and only a small amount of a FM impurity phase ( $\leq 0.5\%$ ). This low AS value, determined by x-ray diffraction, was obtained by a careful control of the synthesis conditions (thermal treatment at 1200 °C for 12 h in 5%  $\text{H}_2/\text{Ar}$ ), as described in Ref. 3. Preparation of Fe impurities free samples is not an easy task since the very stable  $\text{SrMoO}_4$  phase is readily formed above 800 K under the presence of even small  $\text{O}_2$  traces in the processing or measuring atmosphere<sup>7</sup> and thus, severe reducing conditions are required.

We have measured  $M(T)$  vs  $H$  for  $300 \text{ K} \leq T \leq 1100 \text{ K}$  and for  $H \leq 12.5 \text{ kG}$ , with a Faraday balance magnetometer. The measurements were made in air ( $p < 1$  torr). In order to control the reversibility, particularly in the high-temperature range, we increased  $T$  in 20 K steps, repeating the measurements at 473 K after each step. By following this procedure we found irreversible changes for  $T > 800 \text{ K}$ . Thus, we considered reliable only the measurements in the range 300–800 K and we analyze these data. The ESR experiments were performed with a Bruker spectrometer operating at 9.5 GHz between 300 K and 600 K.

In Fig. 1 we show isotherms  $M$  vs  $H$ . For  $T > 450 \text{ K}$  and high magnetic fields, we observed a linear dependence:  $M(T) = M_0(T) + \chi(T)H$ . The parameters obtained for  $H > 5 \text{ kG}$ , are given in Fig. 2. The high-field differential susceptibility,  $\chi(T)$  follows a CW law for  $T > 500 \text{ K}$  and up to 800 K, the limit of the reversible behavior. The fast increase of  $M_0(T)$  at low  $T$  indicates the FM transition at  $T_c = 400 \text{ K}$ , determined from an Arrott plot (see inset in Fig. 1). We note the presence of only a small ferromagnetic component well above  $T_c$ . This contribution is weakly  $T$  dependent and varies between  $M_0(500 \text{ K}) = 0.021 \mu_B/\text{f.u.}$  and  $M_0(800 \text{ K}) = 0.013 \mu_B/\text{f.u.}$ . This result is compatible with the presence of tiny amounts of Fe impurities, as observed by x-ray photoelectron spectroscopy in epitaxial layers<sup>8</sup> of  $\text{Sr}_2\text{FeMoO}_6$ .

The ESR spectrum consists of a single line with Lorentzian shape and  $g = 2.01(2)$  for  $T \geq 430 \text{ K}$  as described in a

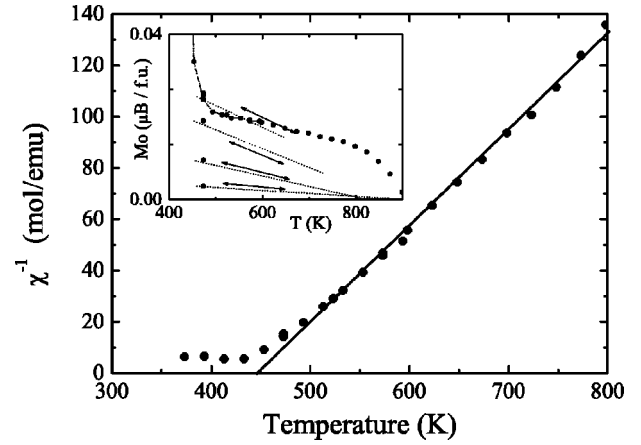


FIG. 2.  $\chi^{-1}$  vs  $T$ . Inset:  $M_0$  vs  $T$ .

preliminary report.<sup>9</sup> Above 450 K the line broadens rapidly and we show in Fig. 3 the peak-to-peak linewidth,  $\Delta H_{pp}(T)$ . The relative double integrated intensity of the line,  $I_{ESR}$ , decreases with increasing temperature, as shown in the inset.

Since the spectrum broadens rapidly with increasing  $T$ , it is important to separate the contribution of the impurities, observed at high temperatures as a  $T$ -independent secondary line.<sup>9</sup> In order to obtain accurate values for  $\Delta H_{pp}(T)$  and  $I_{ESR}(T)$  of the principal line, we have separated the two contributions, for all temperatures above 480 K, by subtracting the impurity spectrum that is almost temperature independent ( $M_0$  varies less than 5% between 480 K and 550 K) and the only visible at  $T > 550 \text{ K}$ .

Important points to elucidate are the magnetic moment of the Fe ions and the possible existence of a measurable Pauli contribution to the PM susceptibility. We have determined separately at each temperature the FM contribution,  $M_0(T)$ , and the true PM susceptibility,  $\chi(T)$ , see Fig. 2. We have found that  $\chi(T)$  can be unambiguously described with a CW law,  $\chi(T) = C/(T - \Theta)$ , with  $C = 2.68(9) \text{ emu K/mol}$  and  $\Theta = 446(3) \text{ K}$ . Any temperature-independent contribution to  $\chi(T)$  associated with the itinerant electrons was smaller than the experimental uncertainty ( $\leq 5 \times 10^{-4} \text{ emu/mol}$ ). The ef-

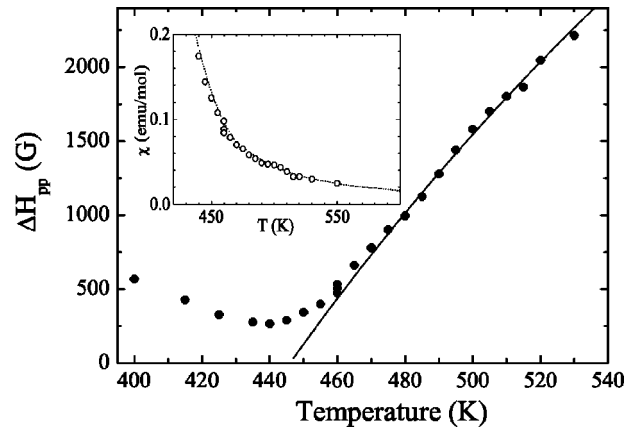


FIG. 3.  $\Delta H_{pp}(T)$  vs  $T$ . The line indicates the fitting with  $\Delta H_{pp}^\infty = 14(1) \text{ kG}$ . Inset:  $I_{ESR}(T)$  vs  $T$ , dotted line corresponds to  $\chi(T)$ .

fective moment derived from the Curie constant should be corrected for the existence of AS defects. For low AS concentration, an estimation of this effect may be obtained in a simplified mean-field model, where misplaced Fe ions are strongly AFM coupled to their neighbors in regular sites. The strength of this interaction is approximated by assuming the same coupling constant<sup>10</sup> as in the LaFeO<sub>3</sub> perovskite ( $T_N = 750$  K). This results in the formation of antiferromagnetic clusters around the AS defects, well above  $T_c$ , which reduce the average effective moment of the sample. In our case the correction is  $\approx 2\%$  and  $\mu_{eff} = 4.72\mu_B/\text{f.u.}$

It should be emphasized that the value obtained for  $\mu_{eff}$  is smaller than that expected for either Fe<sup>3+</sup> ( $\mu_{eff} = 5.9\mu_B$ ) or Fe<sup>2+</sup> ( $\mu_{eff} = 4.9\mu_B$ ) ions. Thus, the ionic picture associated with the description of  $\chi(T)$  only in terms of fully localized Fe<sup>3+</sup> (or even Fe<sup>2+</sup>) moments cannot account for the experimental results. At this point we should ask what may be the contribution of the delocalized electrons to  $\chi(T)$ , taking into account their strong coupling with the Fe cores, indicated by the band-structure calculations.<sup>1,4</sup> An appropriate model for this situation was proposed by Vonsovky and Zener,<sup>11</sup> describing the system in terms of localized ( $M_S$ ) and mobile ( $M_e$ ) electrons in a mean-field approximation.

$$M_e = \chi_e^0(T)H_e^{eff} = \chi_e^0(T)(H + \lambda M_S), \quad (1)$$

$$M_S = \chi_S^0(T)H_S^{eff} = \chi_S^0(T)(H + \lambda M_e + \alpha M_S), \quad (2)$$

where  $\chi_S^0$  and  $\chi_e^0$  are the bare susceptibilities, in the absence of interactions, and  $H_e^{eff}$ ,  $H_S^{eff}$  are the effective fields acting on both sublattices. The polarization of the conduction band, induced by the localized moments, is at the heart of this coupling mechanism. This coupling may be either FM or AFM and it is represented by  $\lambda$ . A possible second neighbor Fe<sup>3+</sup>-Fe<sup>3+</sup> superexchange interaction is denoted by  $\alpha$ . Solving Eqs. (1) and (2), the total susceptibility of the coupled system is given by  $\chi(T) = \chi_S(T) + \chi_e(T)$ , where

$$\chi_S(T) = \frac{\chi_S^0[1 + (\lambda - \alpha)\chi_e^0]}{1 - (\alpha\chi_S^0 + \lambda^2\chi_e^0\chi_S^0)}, \quad (3)$$

$$\chi_e(T) = \frac{\chi_e^0(1 + \lambda\chi_S^0)}{1 - (\alpha\chi_S^0 + \lambda^2\chi_e^0\chi_S^0)}. \quad (4)$$

If both  $\chi_e^0$  and  $\chi_S^0$  were Curie-like,  $\chi(T)$  would have a typical ferrimagnetic behavior. However, one of the coupled systems is delocalized and, therefore, its bare susceptibility  $\chi_e^0$  is temperature independent. In this case, the total susceptibility, for  $\chi_S^0 = C_S/T$  with  $C_S = \mu_S^2 N_A / 3k_B$ , may be written as

$$\chi(T) = \chi_S(T) + \chi_e(T) = \chi_e^0 + \frac{C'}{T - \Theta}. \quad (5)$$

Here, two terms can be identified. The first, temperature independent, is equal to  $\chi_e^0$ . The second one is CW-like, where the Curie constant is now  $C' = C_S(1 + \lambda\chi_e^0)^2$ , renor-

malized because of the  $S$ - $e$  coupling. The effective moment of the coupled system is then given by  $\mu_{eff} = \mu_S(1 + \lambda\chi_e^0)$ . Therefore, we note that a reduction of  $\mu_{eff}$  is expected for  $\lambda < 0$ , due to the AFM coupling of the itinerant electrons to the localized Fe cores. The Curie-Weiss temperature in Eq. (5) is given by  $\Theta = C_S(\lambda^2\chi_e^0 + \alpha)$  and describes an effective interaction between the  $S$  moments mediated by the delocalized electrons. Independently of the sign of  $\lambda$ , and for small  $\alpha$ , it is *always* FM. In the double perovskite structure,  $\alpha$  would be originated in superexchange interactions between second neighbors Fe ions and it is indeed expected to be small.

The behavior predicted by Eq. (5) is consistent with our experimental results, provided  $\chi_e^0$  is below the experimental resolution. Based on the band-structure calculations, and the XAS results<sup>4</sup> we can safely assume a  $3d^5$  configuration for the localized Fe cores, and then  $\mu_S = 5.9\mu_B$ . From the measured  $\mu_{eff} = 4.72\mu_B$  and  $\Theta = 446$  K, we derive  $\chi_e^0 = 3.7 \times 10^{-4}$  emu/mol and  $\lambda = -540$  mol/emu. The value obtained in this way for  $\chi_e^0$  is, then, fully compatible with our dc susceptibility measurements. It is interesting to compare  $\chi_e^0$  with available information in order to test its significance. The corrections for the Landau diamagnetism to the Pauli susceptibility and the Stoner amplification parameter may be derived by comparison between measured and calculated values in other metallic perovskites, such as<sup>12</sup> LaNiO<sub>3</sub>. By doing this we can estimate a density of states at the Fermi level,  $N(\varepsilon_F) = 2.8$  states/eV f.u. for Sr<sub>2</sub>FeMoO<sub>6</sub>. Interestingly enough this value compares well with band-structure calculations. With respect to  $\lambda$ , its negative value confirms the *antiferromagnetic* coupling between the Fe cores and the delocalized electrons at variance with the double exchange mechanism where localized and itinerant spins tend to be parallel. This result supports the mechanism, kinetically driven, described by Sarma *et al.*<sup>4</sup> It should be emphasized that, unlike typical ferrimagnets, the CW temperature is positive, in spite of the AFM character of the interaction. Notice that  $\Theta$ , and consequently  $T_c$ , is proportional to  $\chi_e^0$ . Within this picture a larger density of states at the Fermi level should promote a higher  $T_c$ .

We can now turn to the ESR results. We have found that  $I_{ESR}(T)$  follows the same temperature behavior as  $\chi(T)$ , in the whole PM region (see inset of Fig. 3). This observation indicates that the same magnetic species contributes to the ESR spectrum and the dc susceptibility. Our ESR spectrum should also shed light on the issue of the valence of Fe ions. The measured gyromagnetic factor,  $g = 2.01(1)$ , is  $T$  independent and may be identified with the spin-only ground state of Fe<sup>3+</sup> ions. This resonance corresponds, in the band picture, to the localized  $3d^5$  Fe cores. The observed  $g$  value discards the possibility of assigning the resonance to localized Fe<sup>2+</sup> ( $g \approx 3.4$ ). Our dc susceptibility measurement indicates a strong coupling between these localized Fe cores and the itinerant electrons. The influence of this coupling on the spin dynamics is described by the Bloch-Hasegawa (BH)-type equations.<sup>13</sup>

$$\frac{dM_e}{dt} = \frac{g_e \mu_B}{\hbar} (M_e H_e^{eff}) - \left( \frac{1}{T_{eL}} + \frac{1}{T_{eS}} \right) (M_e - \chi_e^0 H_e^{eff}) + \frac{g_e}{g_S} \frac{1}{T_{Se}} (M_S - \chi_S^0 H_S^{eff}), \quad (6)$$

$$\frac{dM_S}{dt} = \frac{g_S \mu_B}{\hbar} (M_S H_S^{eff}) - \left( \frac{1}{T_{SL}} + \frac{1}{T_{Se}} \right) (M_S - \chi_S^0 H_S^{eff}) + \frac{g_S}{g_e} \frac{1}{T_{eS}} (M_e - \chi_e^0 H_e^{eff}), \quad (7)$$

where  $H_e^{eff}$  and  $H_S^{eff}$ , defined by Eqs. (1) and (2), are now the instantaneous effective fields (including the rf field). Here,  $1/T_{eL}$  and  $1/T_{SL}$  are the spin-lattice relaxation rates for delocalized and localized spins, respectively, and  $1/T_{Se}$ ,  $1/T_{eS}$  the cross-relaxation rates. In our case values of  $g_S$  and  $g_e$  are both expected to be very close to  $g \cong 2$ .

The solutions of Eqs. (6) and (7) present two well-differentiated regimes: bottlenecked and nonbottlenecked, associated with the relative importance of the coupling between the equations.<sup>13</sup> In the nonbottlenecked case both systems tend to respond independently and two resonances should be observed, with  $g$  shifts related to the corresponding effective fields. In the bottleneck limit the strong coupling of Eqs. (6) and (7) results in a single resonance line corresponding to the response of the weighted sum  $M = M_e/g_e + M_S/g_S$  to the rf field (*symmetric mode*). The other solution of the BH equations (*antisymmetric mode*) has no coupling to the rf field and, therefore, does not contribute to the resonance spectrum. The symmetric mode has an effective  $g$  value

$$g = [g_e \chi_e(T) + g_S \chi_S(T)] / \chi(T), \quad (8)$$

where  $\chi_S(T)$  and  $\chi_e(T)$  were defined in Eqs. (3) and (4), respectively, and the linewidth is given by

$$\Delta H_{pp}(T) = \frac{2\hbar}{\sqrt{3} g \mu_B} \left( \frac{\chi_e^0}{\chi(T)} \frac{1}{T_{eL}} + \frac{\chi_S^0(T)}{\chi(T)} \frac{1}{T_{SL}} \right). \quad (9)$$

In our case, where  $g_S \cong g_e$ ,  $M$  is the total magnetization of the system and a temperature-independent  $g \cong 2$  is obtained from Eq. (8). Since  $\chi_S^0(T) = C_S/T \gg \chi_e^0$ , in the whole  $T$  range of our experiment, the linewidth may be approximated by  $\Delta H_{pp}(T) \cong [C_S/[T\chi(T)]] \Delta H_{pp}^\infty$ , where  $\Delta H_{pp}^\infty$ , the linewidth in the high  $T$  limit, is dominated by the relaxation rate of the localized cores,  $1/T_{SL}$ .

We obtained a good fit of the data using a temperature-independent  $\Delta H_{pp}^\infty = 14(1)$  kG, as seen in Fig. 3. The relaxation rate, for strongly localized interacting spins results from the balance between *broadening* (dipolar, antisymmetric exchange, crystal field),  $\omega_a$ , and *narrowing* (isotropic exchange),  $\omega_e$ , interactions between the Fe cores:  $1/T_{SL} \propto (\omega_a^2/\omega_e)$ . The value obtained here for  $\Delta H_{pp}^\infty$  is very large, as compared with those found in other  $\text{Fe}^{3+}$  oxides<sup>10,14</sup> with ordering temperatures around 200–750 K, where  $\Delta H_{pp}^\infty$  varies between 0.5 kG and 1.7 kG. Since we do not expect large variations of  $\omega_a$  in perovskite oxides, we assume that the larger linewidth must be due to a less important degree of exchange narrowing (small  $\alpha$ ).

In CMR manganites, where the conventional double exchange mechanism is responsible for strong FM interactions,

a similar behavior was observed: the increase in the ordering temperature is not accompanied by an enhancement of the exchange narrowing of the ESR line.<sup>15</sup> In the case of  $\text{Sr}_2\text{FeMoO}_6$ , the reason for this behavior can be rationalized in terms of the BH equations. The ordering temperature is determined by the combined effect of the  $S$ - $e$  coupling ( $\lambda$ ) and the  $S$ - $S$  superexchange ( $\alpha$ ). The narrowing of the linewidth, instead, depends only on  $\alpha$ . Taking into account that in the Fe compounds referred before<sup>10,14</sup> the  $\text{Fe}^{3+}$  ions are nearest neighbors it is not surprising that the narrowing effect in  $\text{Sr}_2\text{FeMoO}_6$  is smaller because  $\text{Fe}^{3+}$  ions are second neighbors in this case.

In summary, we have obtained an excellent and consistent description of the experimental results of dc susceptibility and ESR spectroscopy, in terms of a system of two coupled equations for the  $\text{Fe}^{3+}$  localized cores (indicated by  $g \cong 2$ ) and the itinerant electrons, delocalized in both Fe and Mo sites. By solving these equations in a mean-field approximation we can account for the reduction of the effective moment of the  $3d^5$  Fe cores in the PM regime, due to the strong AFM coupling with the itinerant electrons. The delocalized nature of these electrons, with a  $T$ -independent bare susceptibility, causes a nonconventional ferrimagnetic behavior, where  $\Theta$  is positive and equal to  $T_c$ , in spite of the AFM character of the interaction. This is in agreement with the picture presented by Sarma *et al.*<sup>4</sup> Due to the Pauli exclusion principle, the  $t_{2g}$  electrons are allowed to hop from site to site only if the Fe core spins are all oriented antiparallel to them. As a consequence, a FM state with all Fe spins parallel is energetically favored. Within the present framework, the density of states of the mobile electrons, being proportional to  $\chi_e^0$ , plays an important role in the determination of the ordering temperature. The enhancement of  $T_c$  found<sup>16</sup> when double perovskites are electron doped, nicely fits in this model.

Within the same picture we have described the spin dynamics of the strongly coupled system extending the use of the Bloch-Hassegawa equations to materials magnetically concentrated, where  $\chi_S^0(T) \gg \chi_e^0$  even at high temperatures. In this case, the effective relaxation rate for the coupled system is dominated by  $1/T_{SL}$ , the relaxation rate of the localized spins. The absence of narrowing effects associated with the high  $T_c$  is consistent with the fact that the dominant mechanism for magnetic ordering in  $\text{Sr}_2\text{FeMoO}_6$  is a process where the FM coupling between Fe ions is mediated by the mobile electrons.

We thank Dr. B. Alascio for helpful comments. This work was partially supported by CONICET Argentina (PIP 4749), ANPCyT Argentina (PICT 03-05266), and the projects AMORE from the CEE and MAT 1999-0984-CO3 from the CICyT Spain.

- <sup>1</sup>K.-I. Kobayashi, T. Kimura, H. Sawada, K. Terakura, and Y. Tokura, *Nature (London)* **395**, 677 (1998), and references therein.
- <sup>2</sup>C. Ritter, M. R. Ibarra, L. Morellon, J. Blasco, J. García, and J. M. De Teresa, *J. Phys.: Condens. Matter* **12**, 8295 (2000), and references therein.
- <sup>3</sup>Ll. Ballcells, J. Navarro, M. Bibes, A. Roig, B. Martínez, and J. Fontcuberta, *Appl. Phys. Lett.* **78**, 781 (2001).
- <sup>4</sup>S. Ray, A. Kumar, D. D. Sarma, R. Cimino, S. Turchini, S. Zennaro, and N. Zema, *Phys. Rev. Lett.* **87**, 097204 (2001); D. D. Sarma, *Curr. Opin. Solid State Mater. Sci.* (to be published); D. D. Sarma, Priya Mahadevan, T. Saha-Dasgupta, Sugata Ray, and Ashwani Kumar, *Phys. Rev. Lett.* **85**, 2549 (2000).
- <sup>5</sup>D. Niebieskikwiat, R. D. Sánchez, A. Caneiro, L. Morales, M. Vásquez-Mansilla, F. Rivadulla, and L. E. Hueso, *Phys. Rev. B* **62**, 3340 (2000).
- <sup>6</sup>J. Navarro, Ll. Balcells, B. Martínez, and J. Fontcuberta, *J. Appl. Phys.* **89**, 7684 (2001); B. Martínez, J. Navarro, Ll. Ballcells, and J. Fontcuberta, *J. Phys.: Condens. Matter* **12**, 10 515 (2000).
- <sup>7</sup>D. Niebieskikwiat, A. Caneiro, R. D. Sánchez, and J. Fontcuberta, *Phys. Rev. B* **64**, 180406 (2001).
- <sup>8</sup>J. Fontcuberta (private communication).
- <sup>9</sup>M. T. Causa, A. Butera, M. Tovar, and J. Fontcuberta, *Physica B* (to be published).
- <sup>10</sup>R. D. Sánchez (unpublished); R. D. Sánchez, R. E. Carbonio, and M. T. Causa, *J. Magn. Magn. Mater.* **140-144**, 2147 (1995), and references therein.
- <sup>11</sup>S. V. Vonsovsky, *J. Phys. (Moscow)* **10**, 468 (1946); C. Zener, *Phys. Rev.* **81**, 440 (1951).
- <sup>12</sup>R. D. Sánchez, M. T. Causa, J. Sereni, M. J. Sayagués, M. Vallet-Regí, and J. M. González-Calbet, *J. Alloys Compd.* **191**, 287 (1993).
- <sup>13</sup>S. E. Barnes, *Adv. Phys.* **30**, 801 (1981).
- <sup>14</sup>M. T. Causa, R. D. Zysler, M. Tovar, M. Vallet-Regí, and J. M. González-Calbet, *J. Solid State Chem.* **98**, 25 (1992); M. T. Causa, M. Tovar, X. Obradors, A. Labarta, and J. Tejada, *Phys. Rev. B* **44**, 4455 (1991).
- <sup>15</sup>D. L. Huber, G. Alejandro, A. Caneiro, M. T. Causa, F. Prado, M. Tovar, and S. B. Oseroff, *Phys. Rev. B* **60**, 12 155 (1999).
- <sup>16</sup>J. Navarro, C. Frontera, Ll. Balcells, B. Martinez, and J. Fontcuberta, *Phys. Rev. B* **64**, 092411 (2001).